Hemorrhage-induced intestinal damage is complement independent in Helicobacter hepaticus infected mice

Diana J. Hylton, Lauren M. Phillips, Sara M. Hoffman, and Sherry D. Fleming

Published Version Information

Citation: Hylton, D. J., Phillips, L. M., Hoffman, S. M., & Fleming, S. D. (2010). Hemorrhage-induced intestinal damage is complement-independent in Helicobacter hepaticus-infected mice. Shock, 34(5), 467-474.

Digital Object Identifier (DOI): doi:10.1097/SHK.0b013e3181dc077e

Publisher's Link:
http://journals.lww.com/shockjournal/Fulltext/2010/11000/Hemorrhage_Induced_Intestinal_Damage_is.6.aspx

Hemorrhage-induced intestinal damage is complement independent in *Helicobacter-hepaticus* infected mice

Diana J. Hylton[2], Lauren M. Phillips[2], Sara M. Hoffman and Sherry D. Fleming[1]

Affiliations: Division of Biology, Kansas State University, Manhattan, KS 66506

Running head: *H. hepaticus* alters intestines during hemorrhage

This work was supported by NIH Grants AI061691, P20 RR017686 and RR016475 from the Institutional Development Award (IDeA) Program of the NCRR, Dept of Defense grant W81XWH-06-1-0561, HHMI Undergraduate Science Educational Grant and Mark Chapman Scholarship.

[1]Corresponding Author:

Sherry D. Fleming, Ph.D.
18 Ackert Hall
Kansas State University
Manhattan, KS 66506
785-532-6130 (voice)
785-532-6653 (fax)
sdflemin@ksu.edu

[2] These authors contributed equally.

ABSTRACT

With over half of the world population infected, *Helicobacter* infection is an important public health issue associated with gastrointestinal cancers and inflammatory bowel disease. Animal studies indicate that complement and oxidative stress play a role in *Helicobacter* infections. Hemorrhage induces tissue damage which is attenuated by blockade of either complement activation or oxidative stress products. Therefore, we hypothesized that chronic *Helicobacter hepaticus* infection would modulate hemorrhage-induced intestinal damage and inflammation. To test this hypothesis, we examined hemorrhage-induced jejunal damage and inflammation in uninfected and *H. hepaticus* infected mice. *H. hepaticus* infection increased hemorrhage-induced mid-jejunal mucosal damage despite attenuating complement activation. In addition, infection alone increased chemokine secretion, changing the hemorrhage-induced neutrophil infiltration to a macrophage-mediated inflammatory response. The hemorrhage-induced macrophage infiltration correlated with increased secretion of tumor necrosis factor-α (TNF-α[3]) and nitric oxide (NO) in the infected mice. Together these data indicate that *Helicobacter* infection modulates the mechanism of hemorrhage-induced intestinal damage and inflammation from a complement-mediated response to a macrophage response with elevated TNF-α and NO. These data indicate that chronic, low level infections change the response to trauma and should be considered when designing and administering therapeutics.

Key Words: Mouse, nitric oxide, inflammation, macrophage, CD55, jejunum

[3] Non-standard abbreviations: CD55: Decay accelerating factor, DAF; TNF-α: Tumor necrosis factor-alpha; NO: Nitric oxide; CXCL10: Chemokine (C-X-C motif) ligand 10; CCL3: C-C motif chemokine 3; MIP-1α- Macrophage inflammatory protein α (CCL3); CCL4: C-C

motif chemokine 4; MIP-1β: Macrophage inflammatory protein β (aka CCL3); CXCL1: Chemokine (C-X-C motif) ligand 1; CXCL10: Chemokine (C-X-C motif) ligand 10; IP-10: 10 kDa interferon-gamma-induced protein (CXCL10); IL: Interleukin; KC-Keratinocyte derived protein (IL-8); LTB_4 : Leukotriene B4; LPS: Lipopolysaccharide; IFNγ: Interferon gamma; PCR: Polymerase chain reaction; i.p.: Intraperitoneal injection; PMN: Polymorphonuclear leukocyte; SEM: Standard error of the mean; CVF: Cobra venom factor; TLR: Toll-like receptor

INTRODUCTION

Chronic *Helicobacter* infections are found in over 50% of the adult population in the U.S. and up to 90% of the developing world population (1). As the leading cause of peptic ulcers, chronic *Helicobacter pylori* infection is also implicated in gastrointestinal cancer and inflammatory bowel disease (1). Recent studies associated other *Helicobacter* species with liver and colonic diseases including ulcerative colitis, inflammatory bowel disease and Crohn's disease (2). Similar to human diseases, *Helicobacter hepaticus* frequently remains undetected but can cause hepatitis in addition to the above mentioned diseases (3).

Helicobacter-induced colonic inflammation involves significant inflammation which is characterized by chemokine and cytokine production. Recent studies indicate that *Helicobacter* infections increase intestinal secretion of chemotactic factors CXCL10, CCL,3 CXCL2 and interleukin 8 (IL-8) or the murine homolog keratinocyte factor (KC) (3, 4). These chemokines recruit both neutrophils and macrophages. Other studies determined that *Helicobacter* infection increases cytokine expression by both leukocytes and gastric epithelium (5, 6). Specifically, *H. hepaticus* increases tumor necrosis factor-α (TNF-α) and nitric oxide (NO) in the colon of infected, antibody-deficient, Rag-$1^{-/-}$ mice and in the liver of complement deficient mice (7, 8). However, after *H. hepaticus* infection, wildtype C57Bl/6 mice maintain cecal homeostasis with a decreased IL-12 response (5). Despite the apparent resistance, colonic dendritic cells from *H. hepaticus* infected, C57Bl/6 mice differed from uninfected mice when further stimulated with *E. coli* LPS (9). In response to herpes simplex virus type I, *Helicobacter*-infected mice also tended to have fewer IFNγ producing CD8+ T cells in the tracheobronchial lymph nodes (9). Thus, despite no clinical signs of *Helicobacter* infection, the inflammatory response to subsequent

stimulation differs in infected animals.

The *Helicobacter*-induced inflammatory response also includes complement activation. Complement activation is critical to gastric inflammation during *Helicobacter felis* infection, as complement depletion with either cobra venom factor (CVF) or treatment with anti-C5 monoclonal antibody attenuates gastritis (10). However, complement regulatory proteins on the mucosal surface prevent complement-mediated tissue damage and also appear to have a role in *Helicobacter* infections. Expression of complement inhibitor CD55 (Decay Accelerating Factor; DAF) increases on the gastric epithelium of humans colonized with *H. pylori* (11). In addition, the absence of DAF diminishes the *Helicobacter*-induced neutrophil infiltration and inflammatory response (11). These data suggest that both complement activation and expression of complement inhibitors are affected by *Helicobacter* infection.

As the primary cause of trauma-related morbidity and mortality, hemorrhage and the accompanying hemorrhagic-shock result in significant clinical complications due to hypoxic conditions and an excessive immune response (12, 13). Because the splanchnic circulation receives 25-30% of the total blood volume, decreased systemic perfusion during hemorrhage results in lower intestinal blood flow, vasoconstriction and mucosal damage (14). Hemorrhage and hemorrhagic-shock cause intestinal damage and inflammation in a neutrophil and complement-dependent manner (14-16). Although oxidative stress and complement activation prevent bacterial infections, these molecules mediate tissue damage and inflammation when activated excessively. Early changes in cytokine production indicate activation of the systemic inflammatory response during hemorrhagic shock and/or the presence of bacterial DNA (17).

Because cytokines, chemokines, oxidative stress and complement activation are critical in both infection and hemorrhage, we tested the hypothesis that chronic *Helicobacter* infection modulates mucosal damage and inflammation in a fixed-volume mouse model of hemorrhage.

Our data demonstrate that *Helicobacter* infection significantly increases the chemotactic factors KC, CCL3 (MIP-1α), CCL4 (MIP-1β) and CXCL10 (IP-10) in the mid-jejunum. Additionally, complement inhibitor CD55 expression increases in the jejunum, despite the absence of *H. hepaticus* DNA. Consequently, complement activation does not play a role in the hemorrhage-induced, jejunal inflammation and tissue damage in *H. hepaticus* infected mice. Rather, in chronic *Helicobacter* infection, hemorrhage induces an influx of macrophages and TNF-α and NO secretion in the jejunum. Thus, although the specific bacterial mechanism is unknown, a chronic *H. hepaticus* infection in the liver and colon alters the mechanism of hemorrhage-induced damage within the jejunum.

Materials and Methods:

Mice: C57Bl/6 male mice (6-8 wks old) were bred and maintained at Kansas State University. All mice were housed in a 12-hour light-to-dark, temperature-controlled room and allowed food and water ad libitum. Uninfected mice were maintained under specific pathogen free conditions (*Helicobacter* species, mouse hepatitis virus, minute virus of mice, mouse parvovirus, Sendai virus, murine norovirus, *Mycoplasma pulmonis*, Theiler's murine encephalomyelitis virus, and endo- and ecto-parasites). All research was approved by the Institutional Animal Care and Use Committee and conducted in compliance with the Animal Welfare Act and other Federal statutes and regulations concerning animals.

***Helicobacter* Infection:** Separately housed C57Bl/6 male mice were naturally colonized with *H. hepaticus* either by being reared by an infected female or by contact with infected feces during normal grooming. The presence of *H. hepaticus* was verified by PCR analysis of the feces from each infected mouse (data not shown). Fecal DNA was purified using the Qiagen DNA Stool mini kit according to the manufacturer's protocol and PCR amplified for 35 cycles at 54^{o}C using *Helicobacter* specific 16s rRNA primers: forward 5'ATG GGT AAG AAA ATA GCA AAA AGA TTG CAA3' and reverse 5'CTA TTT CAT ATC CAT AAG CTC TTG AGA ATC 3'. PCR products were imaged using AlphaImager (Alpha Innotech) and semi-quantitative analysis performed using Image J (NIH). Each mouse was infected for a minimum of 4-8 wks prior to hemorrhage. Feces from uninfected mice were also analyzed by PCR with 100% negative results. Liver, cecum and colon DNA was purified by Trizol according to the manufacturer's protocol and similar PCR analysis performed. Preliminary data indicated a constant level of shed bacteria at 1- 2 mo post-infection (data not shown) with *H. hepaticus* DNA was also

detectable in the liver, cecum and colon of all mice. In contrast, *H. hepaticus* DNA was found in the jejunum of only 10% of the infected mice (data not shown).

Hemorrhage Protocol: Mice were anesthetized i.p. with ketamine (16 mg/kg) and xylazine (80 mg/kg) and a drop of 0.5% proparacaine hydrochloride ophthalmic solution was applied to the appropriate eye. The hemorrhage treated mice were subjected to 25% total blood volume removal via the retro-orbital sinus as described previously (15). Blood volume removed was based on mouse weight (grams) and calculated using the following equation (~25% = grams x 0.02) (16). Sham-treated mice were subjected to similar procedures with no blood removal. Hemorrhage treatment was completed within five minutes. Body temperature was maintained at 37° C using a water-circulating heating pad and all procedures were performed with the animals breathing spontaneously. At 1 h, 2 h or 3 h post-hemorrhage, mice were euthanized and 2 cm sections of mid-jejunum tissues collected and used for all further analysis. The jejunum was used since previous studies indicated that hemorrhage induces significant damage within the mid-jejunum (15). For C3 depletion studies, 7 units of cobra venom factor (CVF) (Quidel) was administered i.p. to mice at 24 h and 6 h prior to hemorrhage or Sham treatment.

Intestinal Injury Score, Villus Height/Crypt Depth ratio and PMN infiltration: Formalin fixed mid-jejunal sections were transversely sectioned and stained with hematoxylin and eosin (H&E) for analysis of injury. Injury was scored by an observer unaware of the treatment using a six-tiered scale adapted from Chiu et al. as described previously (15, 18). Briefly, each villus was assigned a score as follows: 0- intact villus with no damage, 1- bulging of the epithelium, 2- Guggenheim's space, 3- visible breakage of the epithelium, 4- exposure of intact lamina propria,

5- exuding of the lamina propria and 6- blood loss and denuding of the lamina propria. The average intestinal injury of each animal was determined by grading 75-150 villi in approximately 2 cm length of intestine. Similarly, the number of neutrophils in at least 20 villi (from crypt to villus tip) per H&E stained slide was counted at 1000X magnification. Villus height/crypt depth ratio of at least 15 individual villi per animal was measured using Metavue computer software on the H&E stained slide at 200X magnification All slides were examined by a blinded observer using a Nikon 80i microscope equipped with a DS Nikon color camera connected to the DS-L2 controller unit.

Cytokine, Chemokine, Leukotriene B_4 and C5a production: *Ex vivo* intestinal supernatants were generated as described previously (15) and used to determine the secretions released in a 20 min period. Briefly, 2 cm mid-jejunal intestinal sections were minced, washed, re-suspended in 37°C oxygenated Tyrode's buffer and incubated for 20 min at 37ºC. Following incubation, the supernatants and tissues were collected and stored at -80ºC until assayed. After overnight digestion in 0.1M NaOH at 37ºC, protein content in the intestinal tissue was determined using a BCA protein assay (Pierce). Cytokine and chemokine concentrations in the intestinal supernatants were determined with a Milliplex MAP kit (Millipore) following the manufacturer's instructions and analyzed using MasterplexQT software (MiraiBio). Leukotriene B_4 (LTB_4) concentrations in the intestinal supernatants were measured using a commercially available enzyme immunoassay kit (Cayman Chemicals). All concentrations were normalized to the total intestinal protein content and reported as pg per mg of intestinal tissue. Sera C5a concentrations were determined by capture ELISA (BD Biosciences).

Nitric oxide synthesis: *Ex vivo* mid-jejunal supernatants generated above were assayed for nitrite as a stable end product of NO and oxygen. Equal volumes of supernatant and Griess reagent were incubated for 15 min prior to spectrophotometrically measuring the A550 as described previously (19). Samples were blanked with Tyrode's buffer and compared to a standard curve of $NaNO_2$.

Immunohistochemistry: After Sham or Hemorrhage (HS) treatment, a 2 cm mid-jejunal section was frozen in O.C.T. freezing medium and stored at -80^{o}C until used. Intestinal cryosections, 6-8μm thick, were fixed in cold acetone. Non-specific binding was blocked using 10% donkey serum or 10% goat serum in PBS. Tissues were stained for C3 or CD55 using a rat-anti-mouse C3 antibody (Hycult Biotechnologies), Armenian hamster-anti-mouse CD55 (Biolegend), followed by an appropriate secondary antibody (Jackson Immunoresearch). Directly conjugated rat-anti-mouse F4/80 (eBioscience), rabbit-anti-mouse iNOS (BD Bioscience) or rat-anti-mouse TNF was used for macrophage detection and colocalization studies. Serial sections stained with isotype control antibodies were used as background. Slides were examined by a blinded observer by fluorescent microscopy using a Nikon 80i fluorescent microscope and images acquired using a CoolSnapCf camera (Photometrics) and MetaVue Imaging software (Molecular Devices). Deposition of C3 was analyzed with Image J software (NIH). After determining the intensity threshold from a positive control, the total positive area of 3-5 photomicrographs per tissue was normalized to the appropriate isotype control. Each treatment group consisted of at least 5 animals.

Statistical Analysis: Data are presented as means ± SEM. Overall differences were determined

by two-way ANOVA. Differences between time points were considered significant if $p \leq 0.05$ as determined by one-way ANOVA with a Newman Keuls post-hoc analysis. Differences between infected and uninfected treatments at specific time points were determined by an unpaired t-test analysis (GraphPad).

RESULTS

Helicobacter infection increases intestinal damage.

To test the hypothesis that chronic *H. hepaticus* infection alters hemorrhage-induced intestinal damage, we subjected uninfected and *H. hepaticus* infected mice to hemorrhage and examined jejunal tissue after 1 h, 2 h or 3 h. As indicated in Figure 1, minimal mucosal damage occurred in uninfected mice (open bars) within 1 h post-hemorrhage (Fig. 1A). In addition, the villi remained tall as indicated by a high villus height/crypt depth ratio (V/C) (Fig. 1B). In contrast, at 2 h post-hemorrhage, uninfected mice exhibited slightly shorter villi and significantly more mucosal damage than Sham mice (Fig. 1A-D). By 3 h post-hemorrhage, intestinal mucosal damage decreased, with villi becoming significantly shorter than untreated mice, indicating sloughing of the villi and beginning of villi restitution in uninfected mice (Fig. 1A, B, E).

Persistent *Helicobacter* infection did not significantly alter the injury score or villus height of Sham mice when compared to uninfected Sham mice (Fig. 1A, B, C, F). Similar to uninfected mice, at 1 h post-hemorrhage infected mice sustained no significant intestinal damage or shortening of the villus height when compared to Sham-treated mice (Fig. 1A, B). However, by 2 h post-hemorrhage, infected mice exhibited significantly increased intestinal damage and decreased villus height when compared to Sham treatment (Fig. 1A, B, F, G). Compared to similarly treated uninfected mice, infection also significantly increased injury scores and shorter villi at 2 h post-hemorrhage (Fig. 1A, B, D, G). Despite a decrease in injury score at 3 h post hemorrhage, the villus height/crypt depth remained similar in infected mice (Fig. 1A, B, H). The lower mucosal injury score in conjunction with low V/C in infected mice at 3 h post-hemorrhage suggested the beginning of intestinal restitution (Fig. 1A, B, E, H). Although intestinal damage

was more severe at 2 h post-hemorrhage, by 3 h post hemorrhage intestinal restitution was apparent in *H. hepaticus* infected mice. These data suggest that damage may occur via a different mechanism.

***Helicobacter* infection increases jejunal chemotactic factors.**

As CCL3 (MIP-1α), CXCL10 (IP-10) (20) and IL-8 (21) are up-regulated in response to infection, we hypothesized that infection may alter the chemotactic secretions and subsequent cellular infiltrate following hemorrhage. To test this hypothesis, we examined the jejunal chemokine production from uninfected and infected mice after Sham or hemorrhage treatment. In uninfected mice, the jejunum produced CCL3, CCL4 (MIP-1β) and KC within 2-3 h post-hemorrhage (Fig. 2A, B, D open bars). However, the T cell chemokine CXCL10 remained unchanged in uninfected mice (Fig. 2C open bars). Thus, hemorrhage rapidly increases chemokines which recruit innate immune cells. In contrast, infection alone (Sham treatment) induced significant increases in all four chemokines (Fig. 2A, B, C, D solid bars). In infected mice, hemorrhage further increased CCL4 and KC concentrations (Fig. 2B, D solid bars).

Leukotriene B_4 (LTB_4) also recruits neutrophils and monocytes. In contrast to the chemokines, the intestines of Sham-treated infected or uninfected mice produced similar LTB_4 concentrations (Fig. 3A). In response to hemorrhage, in uninfected mice LTB_4 significantly increased at 2 h and 3 h post-hemorrhage (Fig. 3A open bars). Infection resulted in maximal LTB_4 production at 2 h post-hemorrhage and was significantly higher than uninfected mice at the same time point (Fig. 3A). In contrast to the uninfected mice, LTB_4 concentrations within the jejunum significantly decreased at 3 h post-hemorrhage in infected mice. Although the time course of LTB_4

production appeared shorter, the 2 h post-hemorrhage increase in LTB_4 did not correlate with the hepatic bacterial load (data not shown), indicating that increased LTB_4 production required both infection and hemorrhage.

Helicobacter infection increases jejunal neutrophil infiltration which is not further increased by hemorrhage.

To determine if the infection-induced chemokines resulted in an increased cellular infiltrate, we quantitated the number of neutrophils in the villi. Hemorrhage induced a low but significant increase in the number of neutrophils by 2 h post-hemorrhage in uninfected mice (Fig. 3B open bars). Correlating with chemokine secretions, Sham-treated jejunal tissue from infected mice contained significantly more neutrophils than similarly treated tissue from uninfected mice. The number of neutrophils was not further elevated by hemorrhage (Fig. 3B solid bars). These data indicate that chronic intestinal infection increased neutrophils in the intestinal villi but hemorrhage did not further increase the neutrophil infiltrate.

Hemorrhage-induced intestinal damage is complement independent in _Helicobacter_-infected mice.

Helicobacter infection and hemorrhage induce opposing effects, with complement activation during hemorrhage and complement inhibition by *Helicobacter* infection (11, 15, 22). To determine if *Helicobacter* infection altered the complement mediated intestinal damage, sera C5a production and C3 deposition on the intestinal tissue was determined. As expected, no C3 deposition was visualized on the intestines of Sham-treated animals in the presence or absence of infection (Fig. 4A). In uninfected animals, hemorrhage induced significant C3 deposition on the

intestinal mucosa by 1 h post-hemorrhage, which decreased with time. In contrast, *Helicobacter* infection attenuated intestinal C3 deposition at all time points examined post-hemorrhage (Fig. 4A solid bars). Quantitation of the deposition verified that infection significantly decreased C3 deposition at 1 h post-hemorrhage when compared to similarly treated uninfected mice. Similarly, in uninfected mice, hemorrhage significantly elevated sera C5a concentrations when compared to sham treatment (Fig. 4B open bars). However, infection attenuated C5a production at all time points following hemorrhage (Fig. 4B solid bars). Since *H. pylori* upregulates CD55 (11), it was possible that *H. hepaticus* also increased expression of the complement inhibitor on intestinal tissue. Immunohistochemistry demonstrated that prior to hemorrhage, mucosal DAF expression increased in infected animals when compared to uninfected animals (Fig. 4C, D). Thus, infection increased intestinal DAF expression and subsequently decreased intestinal C3 deposition and C5a production.

To verify that after infection hemorrhage-induced tissue damage was not complement mediated, we depleted C3 by administration of CVF prior to hemorrhage. As indicated in Fig. 5A (open bars), at 2 h post-hemorrhage, CVF treatment significantly attenuated hemorrhage-induced intestinal damage in uninfected mice. However, intestinal damage remained unchanged after CVF treatment in *H. hepaticus* infected mice (Fig. 5A solid bars). In uninfected mice, CVF returned LTB_4 production to sham treated concentrations (Fig. 5B open bars) but only attenuated hemorrhage-induced LTB_4 production in *Helicobacter*-infected mice (Fig. 5B solid bars). These data indicate that *Helicobacter* infection increases hemorrhage-induced intestinal damage and LTB_4 in a complement-independent manner.

***Helicobacter* infection results in a hemorrhage-induced macrophage response.**

LTB_4, CCL3 and CCL4 not only activate neutrophils, but also induce secretion of pro-inflammatory cytokines from macrophages (23). Therefore, it was likely that infection induced macrophage infiltration and subsequent tissue damage. To test this hypothesis, we examined the hemorrhage-induced macrophage infiltration in the jejunum of infected and uninfected mice. Using F4/80 as a macrophage marker, immunohistochemistry showed few macrophages in the intestinal villi of Sham-treated uninfected mice (0.7 ± 0.3 per villus)(Fig. 6A). Although not significantly different from uninfected mice, intestinal villi from Sham-treated infected mice contained 2.6 ± 0.7 macrophages per villus (Fig. 6B). The number of macrophages per villus (2.2 ± 0.3) increased similarly by 2 h post-hemorrhage in the absence of *Helicobacter* (Fig. 6C). However, the number of macrophages in the villi of infected mice increased significantly (5.4 ± 0.8) by 2 h post-hemorrhage (Fig. 6D).

The increased number of macrophages suggested that additional pro-inflammatory mediators may increase in response to hemorrhage in infected mice. Although hemorrhage did not increase jejunal TNF-α in uninfected mice, hemorrhage induced a 4 fold increase in TNF-α production in *H. hepaticus* infected mice (Fig. 7A). In response to HS, tissue sections from *Helicobacter* infected mice indicated that the infiltrating macrophages expressed TNF. This colocalization was not present in Sham-treated or HS-treated uninfected mice (Fig. 7C). Macrophage activation results in another damaging inflammatory molecule, NO. In infected mice, hemorrhage induced significantly more NO at 2 h and 3 h post-hemorrhage (Fig. 7B). Although iNOS expression colocalized with F4/80 staining, epithelial cells also stained for iNOS expression (Fig. 7D).

Thus, macrophage-secreted TNF-α and NO significantly increased in response to hemorrhage in *Helicobacter*-infected but not uninfected mice.

Discussion

Helicobacter spp commonly cause chronic undiagnosed infections. During *H. pylori* infection the inflammatory response increases similar to hemorrhage (3, 4, 10, 11, 15). Our data indicate that *H. hepaticus* infection increases hemorrhage-induced intestinal secretions and damage with a macrophage infiltration. In contrast, infection prevented hemorrhage-induced complement activation. Thus, a subclinical *H. hepaticus* infection modulates hemorrhage-induced damage within the mid-jejunum of C57Bl/6 mice.

To examine the mechanism of increased hemorrhage-induced intestinal damage in response to *Helicobacter* infection, we compared the jejunal innate immune components. *H. hepaticus* infection alone significantly increased intestinal chemokines and resulted in a low but significantly increased neutrophil infiltration in the jejunum. However, intestinal damage required both infection and hemorrhage, indicating that the neutrophil response in infected mice was not sufficient for tissue damage. In contrast, LTB_4 increased in response to hemorrhage (15) and increased synergistically in response to hemorrhage and infection. Known to recruit neutrophils, monocytes/macrophages, eosinophils and T cells to sites of inflammation (24, 25), LTB_4 did not appear to recruit either the neutrophils or macrophages, as the cellular infiltration preceded the increased eicosanoid production. Previous studies indicated that inhibitors of the 5-lipoxygenase pathway decreased *H. pylori*-induced IL-8 production by both gastric epithelium and macrophage cell lines (26). The current study indicates that *H. hepaticus* increases the mouse homolog of IL-8, KC. However, KC elevation was LTB_4 independent, as infection alone increased the chemokine and infection and hemorrhage synergized to produce maximal LTB_4. Interestingly, LTB_4 secretion was not attenuated after complement depletion suggesting the

involvement of another molecular pathway in the production of LTB_4. One possible pathway includes the Toll-like receptors (TLRs), which are expressed on both macrophages and intestinal epithelial cells. Recent studies indicate that *H. pylori* induction of another eicosanoid, prostaglandin E_2, required TLR2 or TLR9 (27). In addition, prostaglandin E_2 production in response to ischemic conditions requires TLR4 (28).

Multiple lines of evidence indicate a role for complement activation in hemorrhage-induced damage. Use of complement inhibitors, including soluble complement receptor 1 and C5a receptor antagonist, attenuated endothelial and intestinal mucosal damage and inflammation (14, 15). We showed that hemorrhage induces intestinal C3 deposition in uninfected but not infected mice. In addition, depletion of C3 with CVF attenuated hemorrhage-induced damage only in uninfected animals. These results are likely due to *Helicobacter*-induced increased DAF expression. As a natural complement regulatory protein on cellular membranes, DAF accelerates decay of the C3 and C5 convertases resulting in limited complement-mediated tissue damage. Up-regulation of DAF occurs during *H. pylori* infection on gastric epithelial cells (11) similar to increased DAF expression in the mid-jejunum. In another model of intestinal damage, administration of soluble DAF attenuates intestinal and lung damage resulting from ischemic events in other organs (29). Although complement is an innate immune component, recent studies indicate that DAF regulates adaptive immunity by limiting T cell production of IL-2 and IFNγ (30). It is possible that similar attenuation of T cell cytokines occurs in response to hemorrhage during a subclinical infection. Together these data indicate that in mice, *H. hepaticus* infection changes the mechanism of hemorrhage-induced damage by attenuating complement activation.

Despite attenuation of complement-mediated tissue damage in infected mice, hemorrhage induced significantly more intestinal damage (at 2 h post-hemorrhage) compared to uninfected mice. Although the ability of *Helicobacter* to colonize and subsequently modulate the immune response to further stimuli is not fully understood, our data indicate that macrophages, TNF-α and NO may contribute to the response. We demonstrate that hemorrhage induces a significant macrophage infiltration in *Helicobacter*-infected mice, which is not seen in uninfected mice. In addition, immunohistochemistry indicates that the infiltrating macrophages express TNF and iNOS. However, other intestinal cells also express iNOS. Preliminary evidence suggests that both macrophages and intestinal epithelial cells release NO in the jejunum of infected mice after hemorrhage. Excess NO may contribute to the damage of the intestinal tight junctions (31) increasing the risk of sepsis in response to hemorrhage in infected mice. Unlike the *Helicobacter*-resistant C57Bl/6 mice in the current study, epithelial cells and macrophages from *H. hepaticus*-infected, immunocompromised $Rag2^{-/-}$ mice, secreted increased TNF and NO in the urinary tract in the absence of hemorrhage (7). Using inducible NO synthase inhibitors, other studies indicated that NO induces significant intestinal damage in multiple animal models (32, 33). Thus, it is likely that increased macrophage infiltration and subsequent NO and TNF-α production is responsible for the increased intestinal damage in *Helicobacter* infected mice.

Helicobacter bacterial DNA was found in the liver, colon and cecum of infected animals and approximately 10% of infected animals expressed *H. hepaticus* DNA in the jejunum (data not shown). Despite the absence of bacterial DNA in the jejunum, cytokines and chemokines were significantly elevated in all infected Sham-treated mice. The mechanism of this inflammatory

response is currently unknown. However, it is similar to the pathogenesis of upper gastrointestinal tract inflammation in Crohn's disease, which is associated with up-regulation of cytokines and chemokines in the duodenum (34). A possible mechanism involves the transport of bacterial products between organs via the lymph. Previous findings indicate that the presence of bacterial DNA increases the inflammatory response to hemorrhagic shock (17). Thus, in *Helicobacter*-infected mice, bacterial components in the lymph may increase the response to hemorrhage. In addition, the infection-induced, intestinal neutrophils may interact with the hemorrhage-induced macrophage infiltration. This interaction would be similar to shock-activated neutrophils in the lung interacting with alveolar macrophages resulting in an exaggerated inflammatory response (35). Although the exact mechanism is currently unknown, our data indicate that the presence of *Helicobacter* in the liver or colon alters the cytokine and chemokine response in the jejunum after hemorrhage.

In summary, we demonstrated that chronic *H. hepaticus* infection significantly alters the inflammatory response in a fixed volume mouse model of hemorrhage in C57Bl/6 mice. *Helicobacter* infection modulated the hemorrhage-induced pathology by increasing DAF expression on the intestinal mucosa and attenuating complement-mediated tissue damage. The increased tissue damage observed is correlated with a hemorrhage-induced macrophage infiltration not seen in uninfected mice. We demonstrated that significant concentrations of TNF-α and NO accompany the hemorrhage-induced macrophage infiltration into the jejunum of infected mice. Taken together, *H. hepaticus* infection modulates the mechanism of hemorrhage-induced tissue damage and inflammation, such that complement inhibitors are ineffective. These data indicate that chronic, low level infections influence the response to trauma and should be

considered when designing and administering therapeutics.

ACKNOWLEDGEMENTS

The authors thank Dr. Mark Haub for assistance with the luminex studies and T. Moses and M. Pope for their excellent technical assistance. We also thank Dr. Terez Shea-Donohue for critical review of the manuscript.

REFERENCES

1. Malaty HM: Epidemiology of Helicobacter pylori infection. *Best Pract Res Clin Gastroenterol* 21:205-214, 2007.
2. Veijola L, Nilsson I, Halme L, Al-Soud WA, Mäkinen J, Ljungh A, and Rautelin H: Detection of Helicobacter species in chronic liver disease and chronic inflammatory bowel disease. *Ann Med.* 39:554-560, 2007.
3. Myles MH, Livingston RS, and Franklin CL: Pathogenicity of *Helicobacter rodentium* in A/JCr and SCID mice. *Comp Med* 54:549-557, 2004.
4. Chaouche-Drider N, Kaparakis M, Karrar A, Fernandez MI, Carneiro LA, Viala J, Boneca IG, Moran AP, Philpott DJ, and Ferrero RL: A commensal Helicobacter sp. of the rodent intestinal flora activates TLR2 and NOD1 responses in epithelial cells. *PLoS ONE* 4:e5396 doi:5310.1371/journal.pone.0005396, 2009.
5. Myles MH, Dieckgraefe BK, Criley JM, and Franklin CL: Characterization of cecal gene expression in a differentially susceptible mouse model of bacterial-induced inflammatory bowel disease. *Inflamm Bowel Dis.* 13:822-836, 2007.
6. Kullberg MC, Jankovic D, Feng CG, Hue S, Gorelick PL, McKenzie BS, Cua DJ, Powrie F, Cheever AW, Maloy KJ, and Sher A: IL-23 plays a key role in Helicobacter hepaticus-induced T cell-dependent colitis. *J. Exp. Med.* 203:2485-2494, 2006.
7. Erdman SE, Rao VP, Poutahidis T, Rogers AB, Taylor CL, Jackson EA, Ge Z, Lee CW, Schauer DB, Wogan GN, Tannenbaum SR, and Fox JG: Nitric oxide and TNF-alpha trigger colonic inflammation and carcinogenesis in *Helicobacter hepaticus*-infected, Rag2-deficient mice. *Proc Natl Acad Sci U S A* 106:1027-1032, 2009.

8. Ge Z, Sterzenbach T, Whary MT, Rickman BH, Rogers AB, Shen Z, Taylor NS, Schauer DB, Josenhans C, Suerbaum S, and Fox JG: Helicobacter hepaticus HHGI1 is a pathogenicity island associated with typhlocolitis in B6.129-IL10(tm1Cgn) mice. *Microbes Infect* 10:726-733, 2008.

9. Gulani J, Norbury CC, Bonneau RH, and Beckwith CS: The effect of helicobacter hepaticus infection on immune responses specific to herpes simplex virus type 1 and characteristics of dendritic cells. *Comp Med* 59:534-544, 2009.

10. Ismail HF, Zhang J, Lynch RG, Wang Y, and Berg DJ: Role for complement in development of Helicobacter-induced gastritis in interleukin-10-deficient mice. *Infect Immun* 71:7140-7148, 2003.

11. O'Brien DP, Israel DA, Krishna U, Romero-Gallo J, Nedrud J, Medof ME, Lin F, Redline R, Lublin DM, Nowicki BJ, Franco AT, Ogden S, Williams AD, Polk DB, and Peek RM, Jr.: The role of decay-accelerating factor as a receptor for *Helicobacter pylori* and a mediator of gastric inflammation. *J. Biol. Chem.* 281:13317-13323, 2006.

12. Bellamy RF: The causes of death in conventional land warfare:implications for combat casulty care research. *Mil. Med.* 149:55-62, 1984.

13. DeBakey ME, and Simeone FA: Battle injuries of the arteries in World War II: an analysis of 2,471 cases. *Ann. Surg.* 123:534-579, 1946.

14. Fruchterman TM, Spain DA, Wilson MA, Harris PD, and Garrison RN: Complement inhbition prevents gut ischemia and endothelial cell dysfunction after hemorrhage/resuscitation. *Surgery* 124:782-792, 1998.

15. Fleming SD, Phillips LM, Lambris JD, and Tsokos GC: Complement component C5a mediates hemorrhage-induced intestinal damage. *J Surg Res* 150:196-203, 2008.

16. Rajnik M, Salkowski CA, Thomas KE, Li YY, Rollwagen FM, and Vogel SN: Induction of early inflammatory gene expression in a murine model of nonresuscitated, fixed-volume hemorrhage. *Shock* 17:322-328, 2002.

17. Luyer MD, Buurman WA, Hadfoune M, Wolfs T, van't Veer C, Jacobs JA, Dejong CH, and Greve JW: Exposure to bacterial DNA before hemorrhagic shock strongly aggravates systemic inflammation and gut barrier loss via an IFN-gamma-dependent route. *Ann. Surg.* 245:795-802, 2007.

18. Chiu C-J, McArdle AH, Brown R, Scott HJ, and Gurd FN: Intestinal mucosal lesion in low-flow states. *Arch Surg.* 101:478-483, 1970.

19. Fleming SD, Leenen PJ, Freed JH, and Campbell PA: Surface interleukin-10 inhibits listericidal activity by primary macrophages. *J. Leukoc. Biol.* 66:961-967, 1999.

20. Livingston RS, Myles MH, Livingston BA, Criley JM, and Franklin CL: Sex influence on chronic intestinal inflammation in Helicobacter hepaticus-infected A/JCr mice. *Comp Med* 54:301-308, 2004.

21. Crabtree JE: Immune and inflammatory responses to Helicobacter pylori infection. *Scand J Gastroenterol Suppl* 215:3-10, 1996.

22. O'Brien DP, Romero-Gallo J, Schneider BG, Chaturvedi R, Delgado A, Harris EJ, Krishna U, Ogden SR, Israel DA, Wilson KT, and Peek RM, Jr.: Regulation of the Helicobacter pylori cellular receptor decay-accelerating factor. *J Biol Chem* 283:23922-23930, 2008.

23. Fahey TJ, 3rd, Tracey KJ, Tekamp-Olson P, Cousens LS, Jones WG, Shires GT, Cerami A, and Sherry B: Macrophage inflammatory protein 1 modulates macrophage function. *J Immunol* 148:2764-2769, 1992.

24. Ohnishi H, Miyahara N, and Gelfand EW: The role of leukotriene B(4) in allergic diseases. *Allergol Int* 57:291-298, 2008.

25. Aiello RJ, Bourassa P-A, Lindsey S, Weng W, Freeman A, and Showell HJ: Leukotriene B4 Receptor Antagonism Reduces Monocytic Foam Cells in Mice. *Arterioscler Thromb Vasc Biol* 22:443-449, 2002.

26. Park S, Han SU, Lee KM, Park KH, Cho SW, and Hahm KB: 5-LOX inhibitor modulates the inflammatory responses provoked by Helicobacter pylori infection. *Helicobacter* 12:49-58, 2007.

27. Chang YJ, Wu MS, Lin JT, and Chen CC: Helicobacter pylori-Induced invasion and angiogenesis of gastric cells is mediated by cyclooxygenase-2 induction through TLR2/TLR9 and promoter regulation. *J Immunol* 175:8242-8252, 2005.

28. Moses T, Wagner LM, and Fleming SD: Tlr4 mediated cox-2 expression increases intestinal ischemia/reperfusion induced damage. *J. Leukoc. Biol.* 86:971-980, 2009.

29. Weeks C, Moratz C, Zacharia A, Stracener C, Egan R, Peckham R, Moore FD, Jr., and Tsokos GC: Decay-accelerating factor attenuates remote ischemia-reperfusion-initiated organ damage. *Clin. Immunol.* 124:311-327, 2007.

30. Longhi MP, Harris CL, Morgan BP, and Gallimore A: Holding T cells in check--a new role for complement regulators? *Trends Immunol* 27:102-108, 2006.

31. Xu DZ, Lu Q, and Deitch EA: Nitric oxide directly impairs intestinal barrier function. *Shock* 17:139-145, 2002.

32. Ergun O, Ergun G, Oktem G, Selvi N, Dogan H, Tuncyurek M, Saydam G, and Erdener A: Enteral resveratrol supplementation attenuates intestinal epithelial inducible nitric

oxide synthase activity and mucosal damage in experimental necrotizing enterocolitis. *J Pediatr Surg* 42:1687-1694, 2007.

33. Naito Y, Takagi T, Ichikawa H, Tomatsuri N, Kuroda M, Isozaki Y, Katada K, Uchiyama K, Kokura S, Yoshida N, Okanoue T, Yoshikawa T, Suzuki Y, Deitch EA, Mishima S, Lu Q, and Xu D: A novel potent inhibitor of inducible nitric oxide inhibitor, ONO-1714, reduces intestinal ischemia-reperfusion injury in rats. *Nitric Oxide* 10:170-177, 2004.

34. Moriyama T, Matsumoto T, Jo Y, Yada S, Hirahashi M, Yao T, and Iida M: Mucosal proinflammatory cytokine and chemokine expression of gastroduodenal lesions in Crohn's disease. *Aliment Pharmacol Ther* 21 Suppl 2:85-91, 2005.

35. Li Y, Xiang M, Yuan Y, Xiao G, Zhang J, Jiang Y, Vodovotz Y, Billiar TR, Wilson MA, and Fan J: Hemorrhagic shock augments lung endothelial cell activation: role of temporal alterations of TLR4 and TLR2. *Am J Physiol Regul Integr Comp Physiol* 297:R1670-1680, 2009.

FIGURE LEGENDS

Figure 1. *Helicobacter* infection increased intestinal damage at 2 h post-hemorrhage. Mucosal injury (A) and villus height/crypt depth ratio (B) were determined from H&E stained jejunal sections from *Helicobacter*-infected (solid bars) and uninfected (open bars) after Sham or 1, 2 or 3 h post-hemorrhage (HS) treatment.. Each bar is the average ± SEM of 6-10 mice per group. (*) indicates $p \leq 0.05$ compared to respective Sham treatment and (ϕ) indicates $p \leq 0.05$ compared to similar treatment of uninfected animals. C-H) Representative photomicrographs of H&E stained intestinal sections from infected (F, G, H) and uninfected (C, D, E) Sham-treated (C, F), 2 h post-HS treated (D, G) or 3 h post-HS treated (E, H) mice. Original photomicrographs are 200X magnification.

Figure 2. *Helicobacter* infection induced intestinal chemotactic factors. *Ex vivo* jejunal chemokines CCL3 (A), CCL4 (B), CXCL10 (C), and KC (D) produced by intestinal tissue sections from infected (solid bars) and uninfected (open bars) mice subjected to Sham or hemorrhage (HS) treatment were determined by multiplex analysis. Chemokine concentrations were normalized to tissue protein content and expressed as pg per mg of intestinal tissue. Each bar represents the average ± SEM with 4-10 mice per group. (*) indicates $p \leq 0.05$ compared to respective Sham treatment and (ϕ) indicates $p \leq 0.05$ compared to similar treatment of uninfected animal.

Figure 3. Intestinal LTB_4 and neutrophil infiltration are induced by hemorrhage and *Helicobacter* infection. A) *Ex vivo* intestinal LTB_4 production by *Helicobacter*-infected (solid bars) and uninfected (open bars) mice subjected to Sham or hemorrhage (HS) treatment was measured. Each bar represents the average ± SEM with 5-10 animals per group. B) Neutrophils

(PMN) present in villi of each treatment group were counted from formalin fixed H&E stained mid-jejunal intestinal sections at 1000X and are presented as PMN per high powered field. Each bar represents the average of 4-10 animals. (*) indicates $p \leq 0.05$ compared to Sham treatment and (ϕ) indicates $p \leq 0.05$ compared to similar treatment of uninfected animals.

Figure 4. *Helicobacter* infection decreased intestinal C3 deposition and increased DAF (CD55) expression following hemorrhage. Mid-jejunal sections from uninfected (open bars, C) and *Helicobacter*-infected (solid bars, D) C57Bl/6 mice after Sham or hemorrhage (HS) treatment were stained for C3 deposition (A) and DAF expression (C, D). Sera C5a was quantitated by ELISA (B). Each bar represents the average ± SEM of 8-10 mice per group. (*) indicates $p \leq 0.05$ compared to the respective Sham treatment and (ϕ) indicates $p \leq 0.05$ compared to similar treatment of uninfected animals. Original magnification of photomicrographs is 200X.

Figure 5. Cobra Venom Factor (CVF) depletion of C3 did not attenuate hemorrhage-induced jejunal tissue damage in *Helicobacter*-infected mice. After *Helicobacter*-infected (solid bars) and uninfected (open bars) mice were subjected to Sham, or Hemorrhage (HS) in the presence of CVF treatment, mucosal injury (A) or jejunal LTB_4 (B) production were quantitated at 2 hr. Each bar represents the average ± SEM of 6-10 mice per group. (*) indicates $p \leq 0.05$ compared to similar Sham treatment and (ϕ) indicates $p \leq 0.05$ compared to respective uninfected treatment.

Figure 6. Hemorrhage and infection increased F4/80 macrophages in the intestinal villi.

Mid-jejunal tissue sections from uninfected (A, C) and *Helicobacter*-infected (B, D) C57Bl/6 mice after Sham (A, B) or hemorrhage (HS) (C, D) treatment were stained for F4/80. Original magnification of photomicrographs (A-D) is 400X and the inset (D) is enlarged 3 fold. Data are representative of five individual experiments with 3-4 photos per treatment group in each experiment. Bar = 20 μm

Figure 7. *Helicobacter* infection increased jejunal TNF-α and NO production. *Ex vivo* generated mid-jejunal concentrations of TNF-α (A) and nitric oxide (NO) (B) from *H. hepaticus* infected (solid bars) and uninfected (open bars) mice were measured. Each bar represents the average ± SEM with 3-10 mice per group. (∗) indicates $p \leq 0.05$ compared to similar Sham treatment and (ϕ) indicates significant difference ($p \leq 0.05$) compared to similarly treated uninfected mice. (C, D) After hemorrhage, F4/80 (Red) co-localized with TNF-α (C) or iNOS (D) expression (Green) in the mid-jejunum of *Helicobacter*-infected mice.

Figure 1

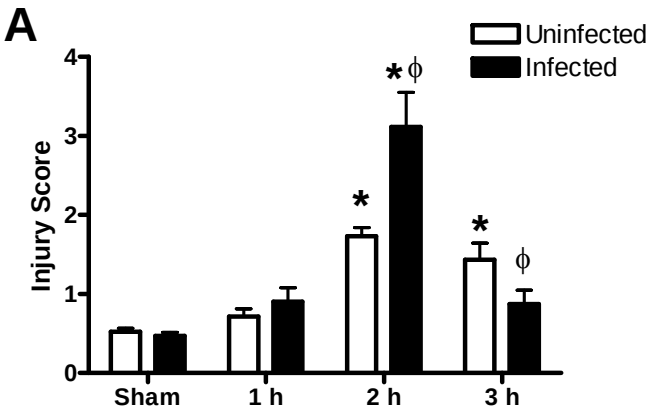
A
Uninfected
Infected
Injury Score
0
1
2
3
4
Sham
1 h
2 h
3 h
*
*ϕ
*
ϕ

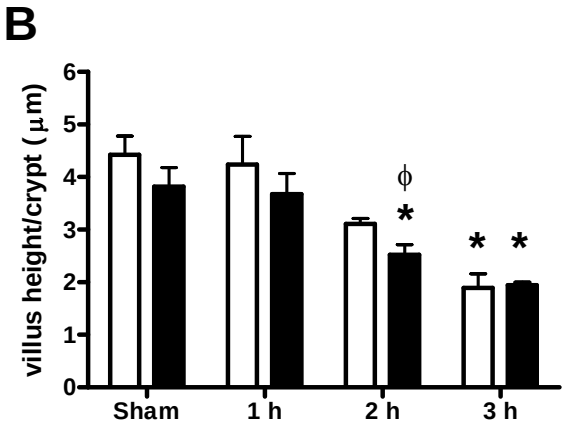
B
villus height/crypt (μm)
0
1
2
3
4
5
6
Sham
1 h
2 h
3 h
ϕ
*
* *

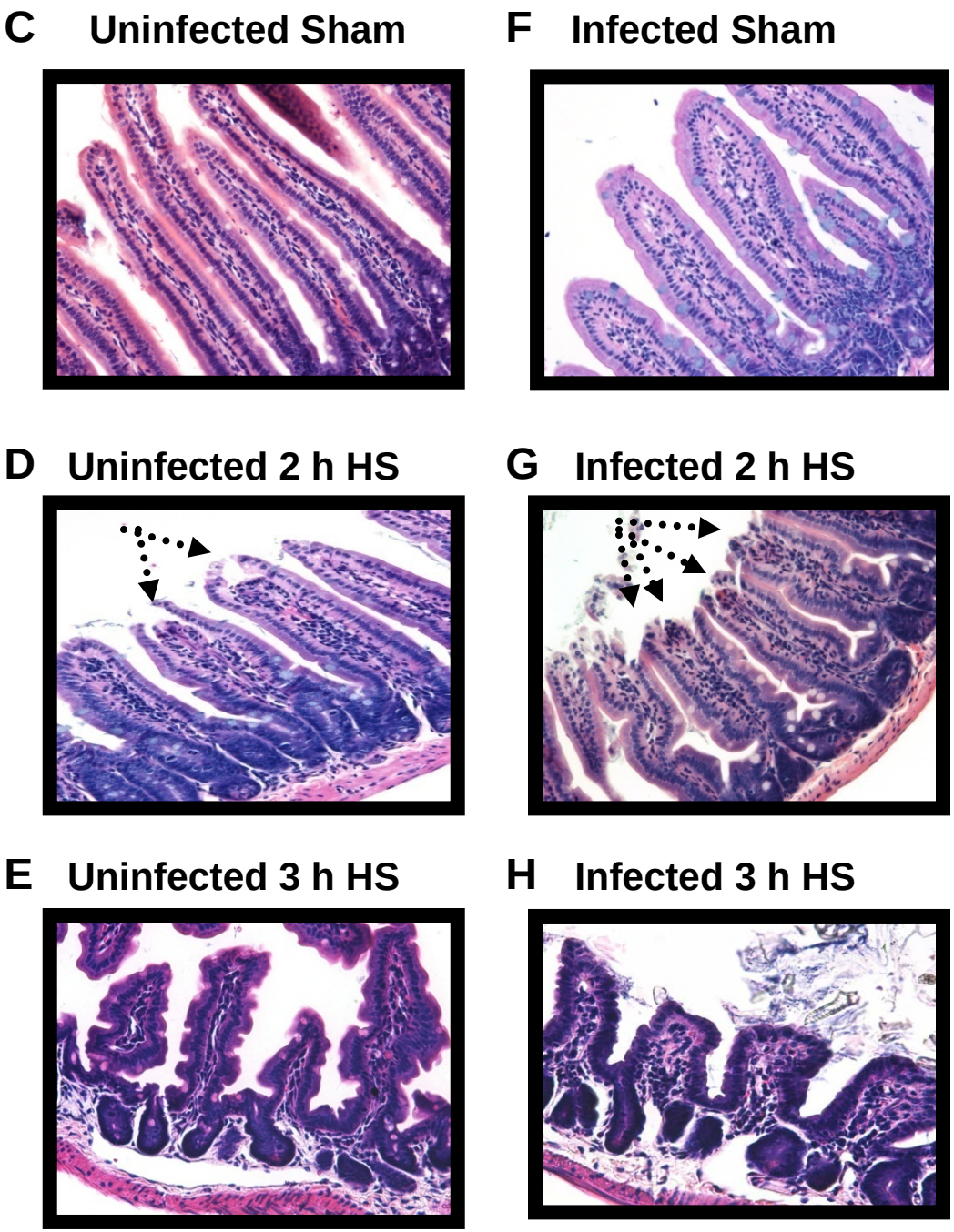
C Uninfected Sham
F Infected Sham
D Uninfected 2 h HS
G Infected 2 h HS
E Uninfected 3 h HS
H Infected 3 h HS

Figure 2

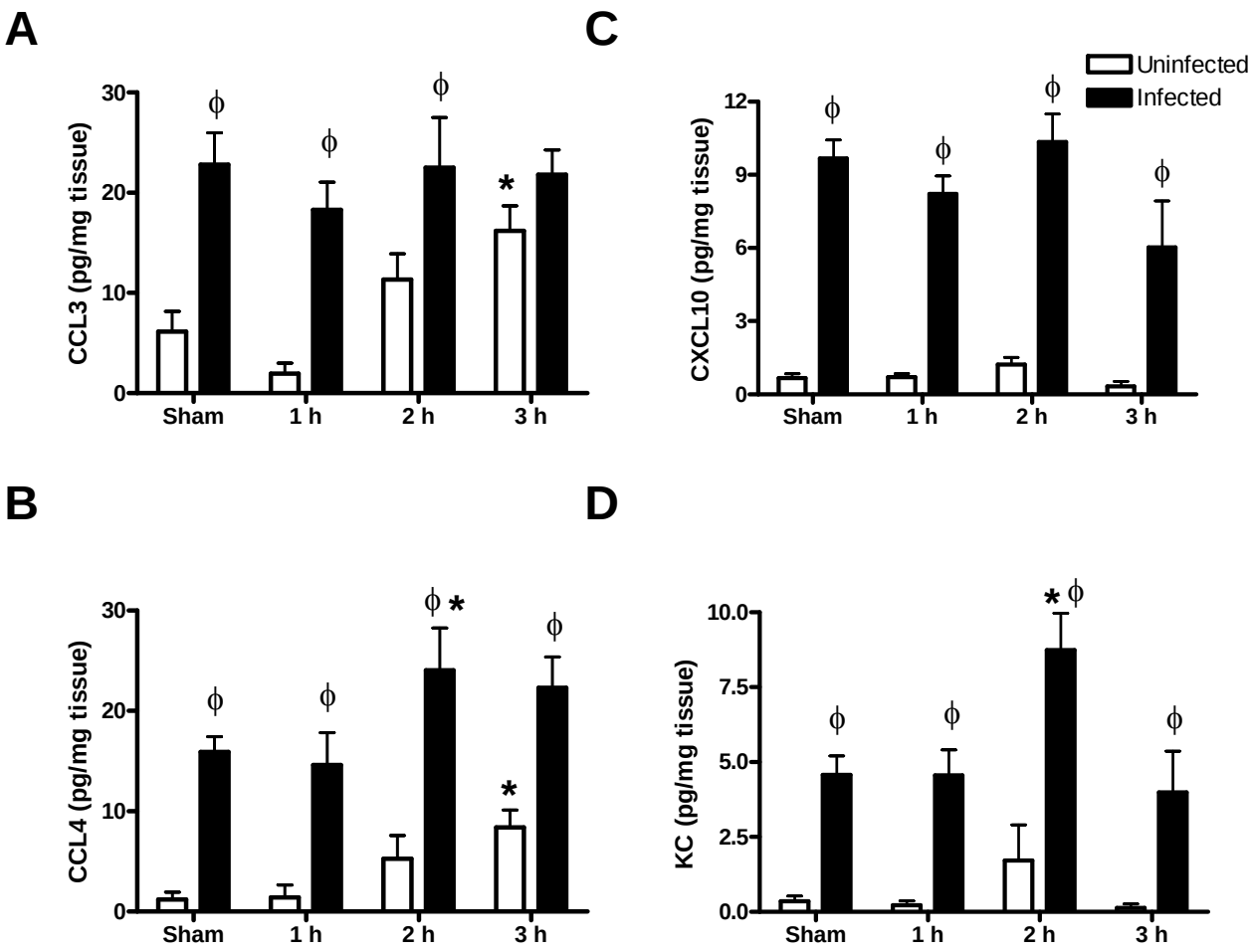
A
B
C
D
CCL3 (pg/mg tissue)
CCL4 (pg/mg tissue)
CXCL10 (pg/mg tissue)
KC (pg/mg tissue)
Uninfected
Infected
Sham
1 h
2 h
3 h
ϕ
*

Figure 3

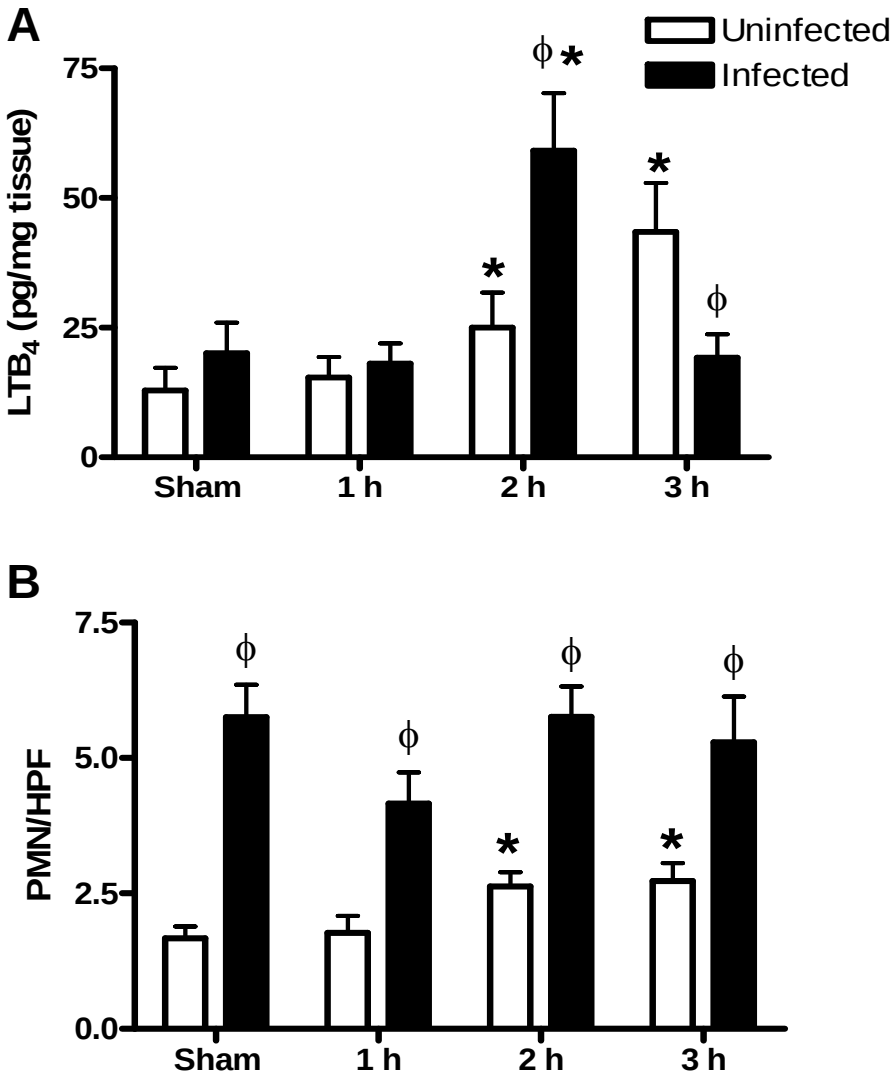
A
Uninfected
Infected
LTB_4 (pg/mg tissue)
75
50
25
0
Sham
1 h
2 h
3 h
B
PMN/HPF
7.5
5.0
2.5
0.0
Sham
1 h
2 h
3 h

Figure 4

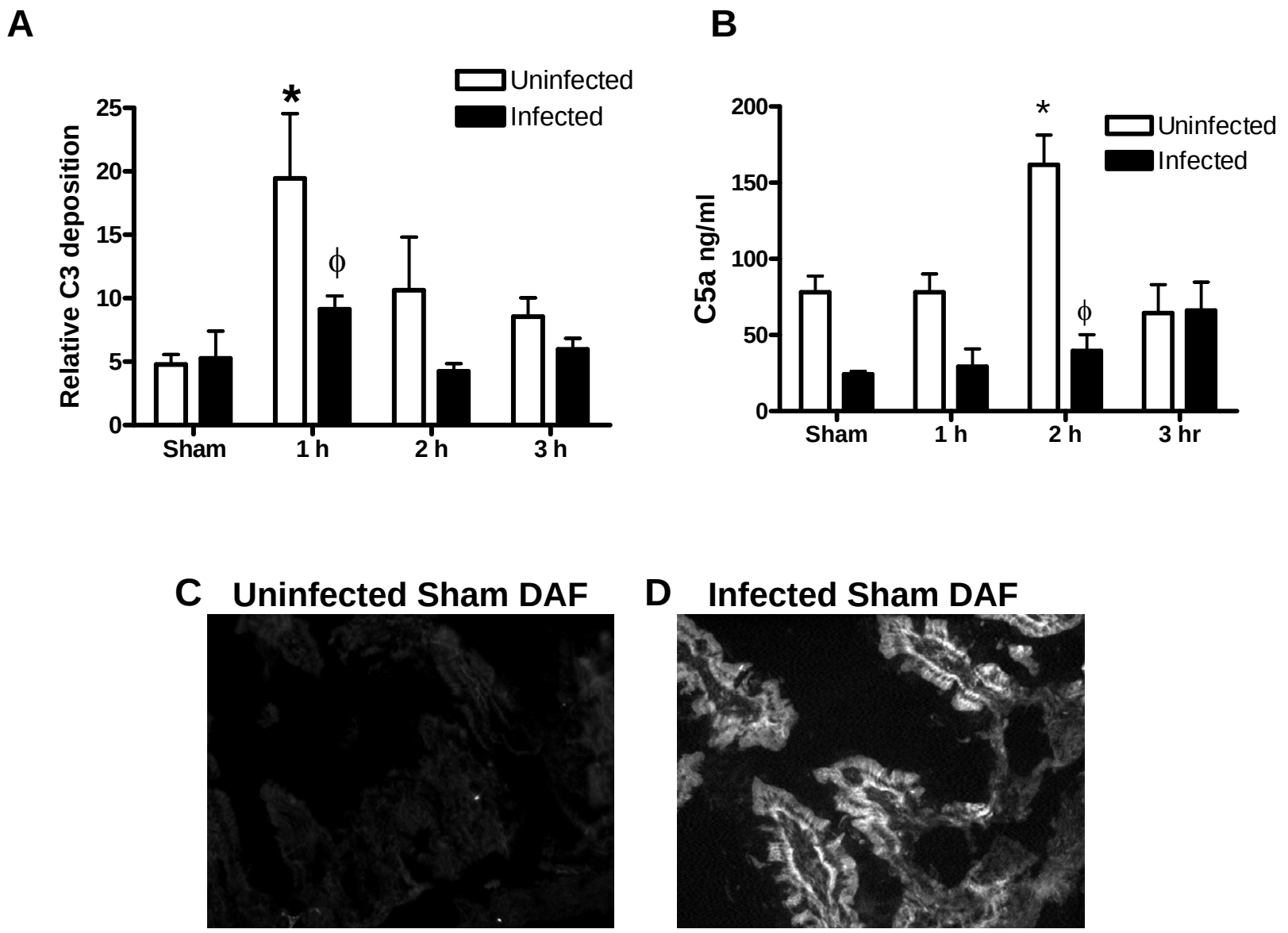
A
Relative C3 deposition
25
20
15
10
5
0
Sham
1 h
2 h
3 h
*
ϕ
Uninfected
Infected
B
C5a ng/ml
200
150
100
50
0
Sham
1 h
2 h
3 hr
*
ϕ
Uninfected
Infected
C Uninfected Sham DAF
D Infected Sham DAF

Figure 5

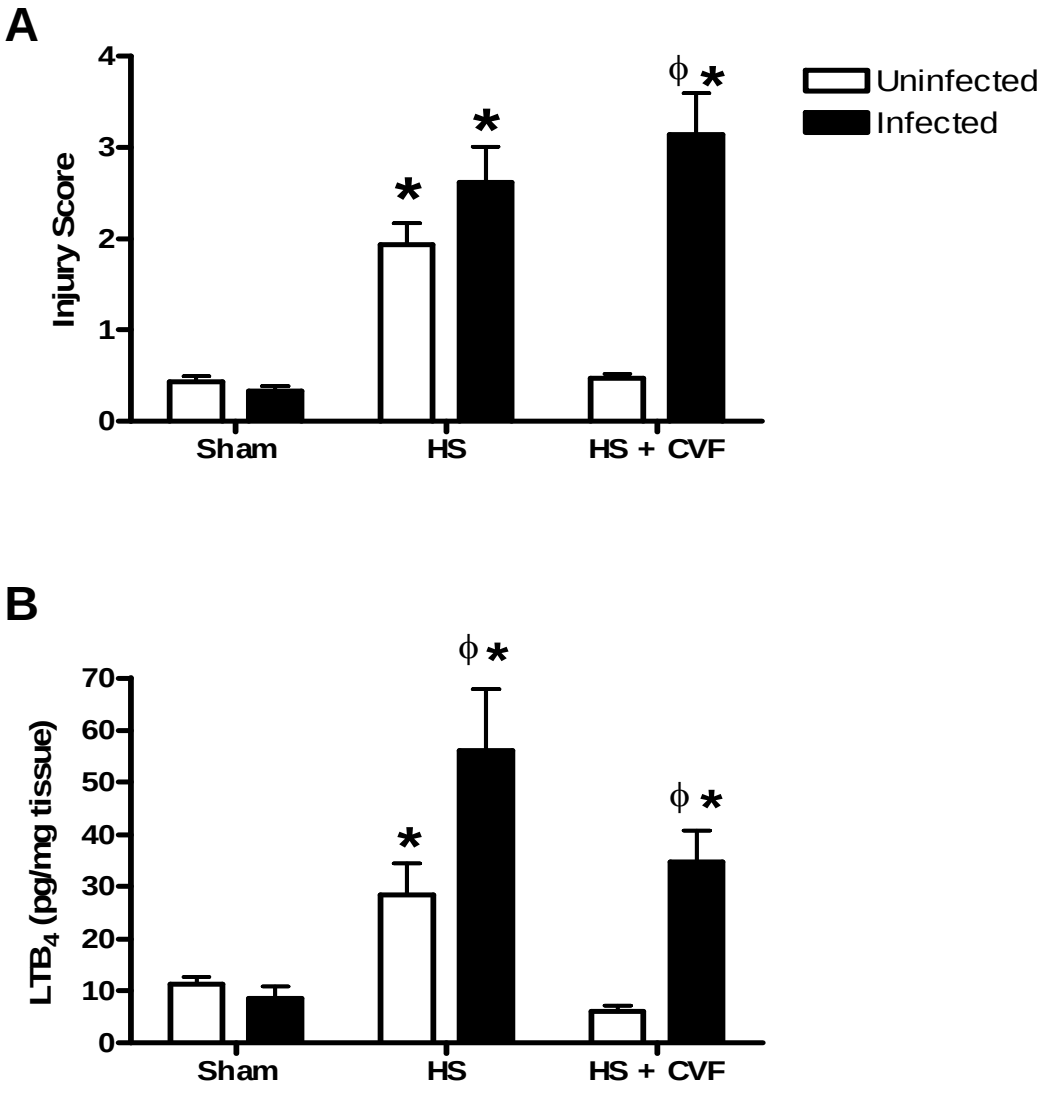
A
Injury Score
0
1
2
3
4
Sham
HS
HS + CVF
*
*
ϕ *
Uninfected
Infected
B
LTB4 (pg/mg tissue)
0
10
20
30
40
50
60
70
Sham
HS
HS + CVF
*
ϕ *
ϕ *

Figure 6

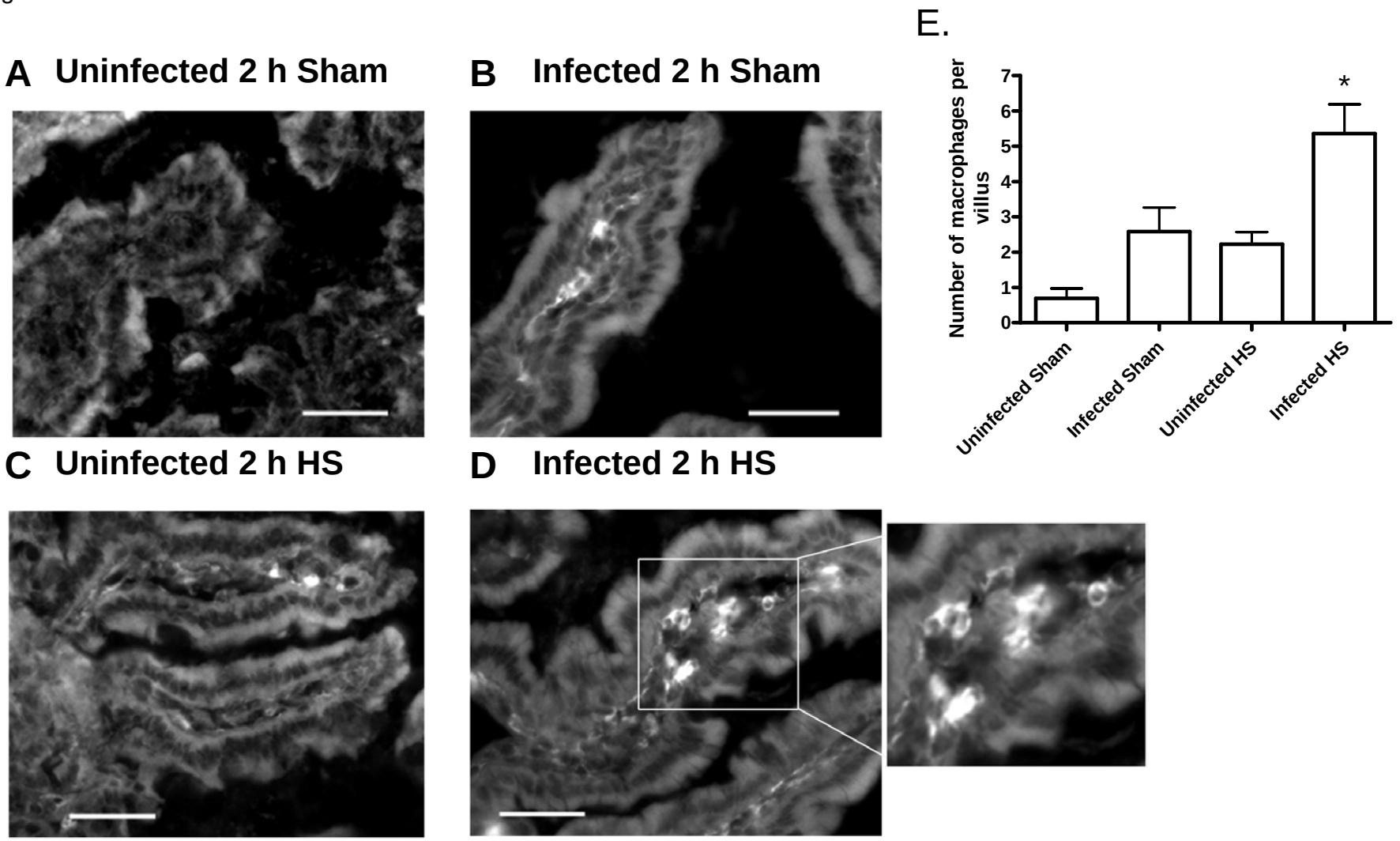
A Uninfected 2 h Sham
B Infected 2 h Sham
C Uninfected 2 h HS
D Infected 2 h HS
E.
Number of macrophages per villus
0
1
2
3
4
5
6
7
*
Uninfected Sham
Infected Sham
Uninfected HS
Infected HS

Figure 7

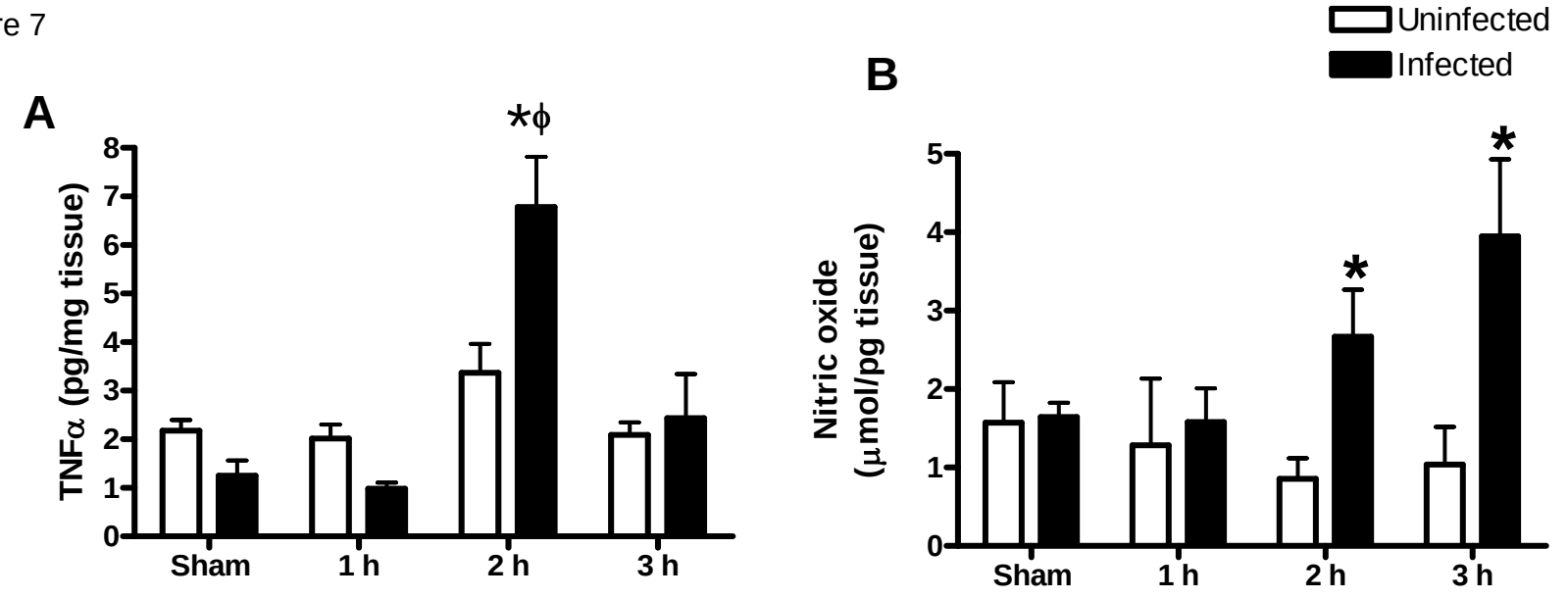

C TNF and F480

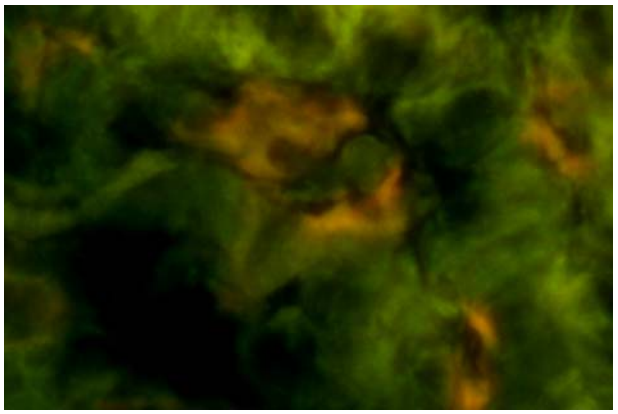

D iNOS and F480